MEASURING PLANKTON DISTRIBUTIONS WITH AN AIRBORNE LIDAR

James H. Churnside

NOAA Earth System Research Laboratory, 325 Broadway, Boulder, CO 80305, USA
E-mail:James.H.Churnside@noaa.gov

ABSTRACT

Traditional techniques for measuring the distribution of plankton are limited by the speed of a ship – typically, 5 m s^{-1} or less. Under these conditions, spatial variability may be difficult to separate from temporal variability if coverage over large areas is desired. Plankton blooms can occur over large areas in a matter of days, so this can be important. In addition, the high cost of research vessels relative to aircraft may make large-scale surveys difficult. For these reasons, we have investigated the possibility of measuring plankton distributions with an airborne LIDAR. During this investigation, we have discovered that plankton layers can also be used to observe hydrodynamic features in the ocean, particularly internal waves.

1. LIDAR DESCRIPTION

The NOAA Fish LIDAR (Fig. 1) is an airborne backscatter LIDAR. [1] The receiver telescope and the laser are mounted side by side, and the system is aimed downward through a hole in the bottom of a small twin-engine aircraft, generally flying at an altitude of 300 m and a speed of about 90 m s^{-1}. To reduce direct surface reflections, the LIDAR is directed at an angle of 15° from nadir.

Fig. 1. Photograph of NOAA Fish LIDAR in NOAA Twin Otter. The rack on the left contains laser power supply and cooling system, computer, and timing electronics. The optics package with laser and receiver is aft of the rack, just to the right in the photo.

The transmitter characteristics are determined by the laser and associated optics. The laser is a Q-switched, frequency-doubled Nd:YAG. It produces about 100 mJ of 532 nm light in a 12 nsec pulse at a repetition rate of 30 Hz. This pulse length produces a measurement volume in the water that is about 1.3 m long. The laser is linearly polarized, and the beam is diverged by a lens in front of the laser. The divergence was chosen so that the irradiance at the sea surface satisfies the U.S. standard for exposure to laser light in the workplace. [2] This is also safe for marine mammals. [3] The diverged beam is directed by a pair of mirrors so that it is parallel to the axis of the telescope.

The receiver collects, filters, and detects the light reflected back to the aircraft. It includes a 17-cm-diameter refracting telescope with a polaroid filter, which is oriented perpendicular to the polarization of the laser. The cross-polarized component was used because it produces the best contrast between fish and smaller scattering particles in the water. This was determined during ship tests of the LIDAR, where the depolarization of the return from fish was about 30% and the depolarization of the water return was only about 10%. [4] We expect that the depolarization from zooplankton would also be larger than the water background, because they are much larger than the wavelength of light and have a shape that is very different from a smooth sphere. The results tend to support this expectation. To reject background light, the light collected by the telescope passes through an interference filter with a bandwidth of 10 nm. Background light is also reduced by an aperture at the focus of the primary lens that matches the field of view of the telescope to the divergence of the transmitted laser beam. The resulting light is incident on a photomultiplier tube (pmt), and the pmt output is logarithmically amplified to increase the dynamic range.

The data-collection computer has several functions. It digitizes and records the log-transformed voltage signal with 8 bits of resolution at a rate of 1 GHz. This sample rate corresponds to a depth resolution of 0.11 m. The computer also records the aircraft position from the GPS, GPS time, the voltage applied to the pmt, and the attitude of the aircraft as measured by tilt sensors and laser gyroscopes on the optical package. The pmt voltage is used to calculate the gain of the tube, which is necessary for calibration. The computer also displays the data in real time during flight.

LIDAR data processing is performed after the flights, and is done in several steps. These include calculation of the depth-dependent photocathode current, estimation of the excess current at each depth, and application of a threshold to estimate the zooplankton return. The excess current is defined as the photocurrent that is in excess of that which would be expected from a homogeneous distribution of scattering particles.

In the first step, the various component gains are used to calculate the photocathode current for each sample, and the time of each sample is converted to a depth in the water column. This step eliminates the effects of changing gain so that all the data are directly comparable. We find the sample that corresponds to the surface by identifying the sample with the largest current, and depth of each sample is found using the 0.11 cm spacing between samples.

The next step in processing is to calculate the excess current for each sample of each return pulse, using a theoretical model of the pulse shape. The backscattered LIDAR power at depth z can be described by the following equation: [1]

$$S(z) = A[\beta_W + \beta_P(z)]\frac{1}{L^2(z)}\exp(-2\alpha z) + B$$

where A is a factor that depends on the system parameters and the geometry, β_W is the backscatter coefficient of the water column not including the plankton component, β_P is the backscatter coefficient of the plankton, L is the optical distance from the aircraft to the measurement depth, α is the LIDAR attenuation coefficient, and B is the background signal level. B, primarily due to skylight reflected from the surface, is measured using the last 100 samples of each pulse, which is after all of the laser photons have been absorbed. The standard deviation of these same samples was used as an estimate of the receiver noise, σ_R, for each pulse.

The quantities $A\beta_W$ and α are found for each LIDAR pulse using the above equation, with several assumptions. The first is that β_W does not vary with depth, so we can perform a 2-point fit to obtain the parameters of interest. The second assumption is that we can find 2 points for which β_P is zero, and the fit is made using these points. One of these points is generally taken to be the surface in calm seas or a depth of around 2 m if there are significant numbers of breaking waves at the surface. The second point is taken to be near the limit of depth penetration of the LIDAR

We then apply a threshold to the LIDAR data to remove small values. That is, we set

$$\beta_P(z) = 0 \quad if \quad S(z) < TA\beta_W\frac{1}{L^2(z)}\exp(-2\alpha z) + B$$

where T is the threshold value. A value of $T = 1$ means that all positive estimates of $\beta_P(z)$ are included; negative values are always very small and are assumed to be due to noise. Generally we set $T = 1$ to retain contributions from very small particles like phytoplankton, and somewhat higher to retain only the contribution from larger particles like zooplankton.

2. ZOOPLANKTON DETECTION

The ability of the LIDAR to detect zooplankton was tested in Prince William Sound, Alaska in the May 2002. [5] Large-bodied (up to several mm) calanoid copepods of the genus *Neocalanus* (Fig. 2) are an important component of the ecology of the Sound. In April and May, these copepods typically form over half

Fig. 2. Photograph of the copepod *Neocalanus*.

of the zooplankton biomass in the Sound. [6] Their large size and high energy content contribute to their importance as a food source for larger animals in the sound. [7,8] The timing of natural pink salmon (*Oncorhynchus gorbuscha*) fry entry into salt water is adapted to match that of the migration of *Neocalanus* to the surface in the spring, [9] and survival and early growth rates of pink salmon are dependent on the availability of *Neocalanus* in the spring. [8]

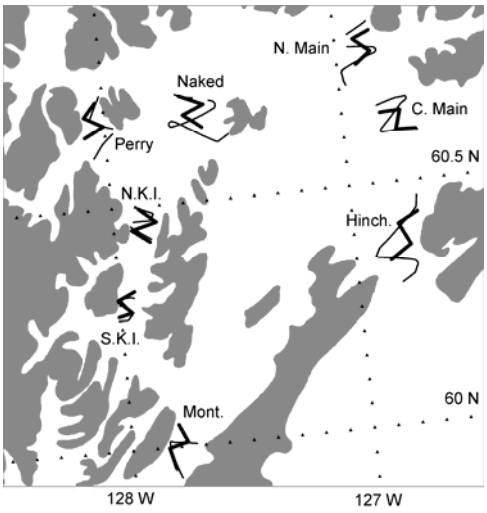

Fig. 3. Map of Prince William Sound, Alaska showing the acoustic (heavy lines) and LIDAR (light lines) survey tracks in each of the 8 areas.

Eight regions in the Sound (Fig. 3) were surveyed by LIDAR and by standard acoustic techniques. With a threshold value of unity, the correlation between the two techniques was low. This is likely due to a large quantity of phytoplankton (diatoms) is the Sound at the same time. The greatest correlation was found for a threshold level of 2.75, which produced a correlation of 0.78, and those values are plotted in Fig. 4.

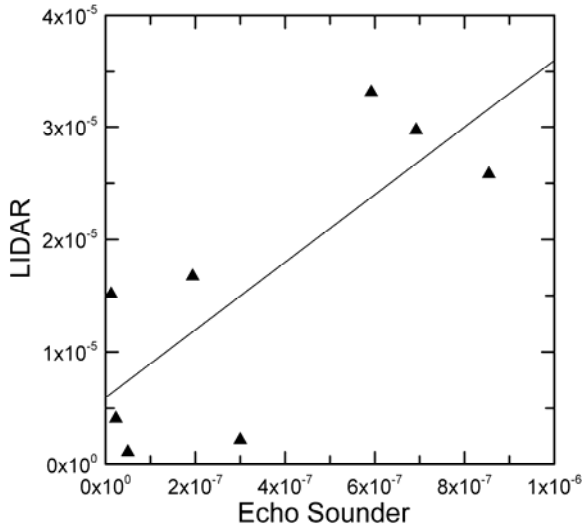

Fig. 4. Plot of LIDAR return as a function of the echo-sounder return for the 8 areas surveyed in Prince William Sound.

3. HYDRODYNAMIC FEATURES

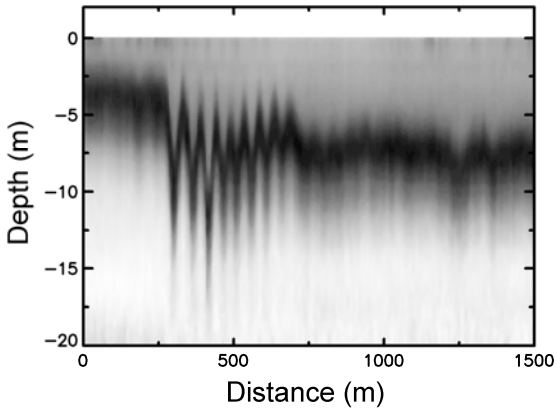

Fig. 5. Intensity of the LIDAR return as a function of depth and relative distance along the flight track showing a strong internal wave perturbing the isopycnal surface.

Plankton layers can also serve as tracers of hydrodynamic features in the ocean. [10] A density gradient can be created in the ocean by, for example, a river outflow that creates a layer of lighter fresh water over heavier salt water or solar heating that creates a layer of lighter warm water over heavier cold water. Gravity waves can propagate on this interface, just as they do at the air/sea density interface. In Fig. 5, one can see the vertical perturbation of a plankton scattering layer in the Gulf of Alaska. This is a

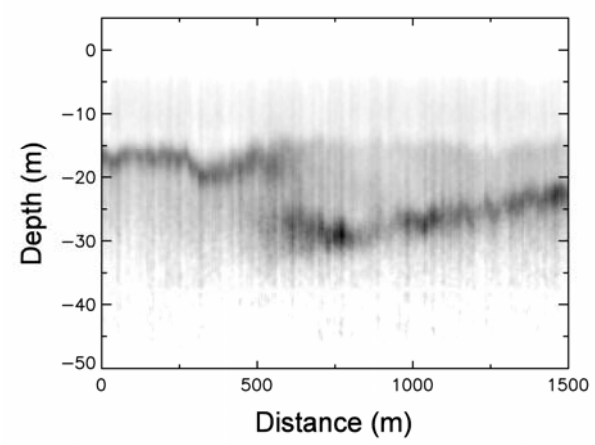

Fig. 6. Intensity of the LIDAR return as a function of depth and distance along the flight track showing a change in the depth of the isopycnal surface of over 10 m.

nonlinear wave train created by the interaction of the tides with the continental shelf. [11] In another example (Fig. 6), a discrete jump in the depth of the isopycnal surface is seen because of its effects on the plankton layer.

4. CONCLUSIONS

From these investigations, we conclude that airborne LIDAR can be a useful tool for investigation of the distribution of plankton in the upper ocean. Both small phytoplankton and larger zooplankton are detectable, and it appears that one can discriminate between them by the judicious application of a level threshold to the data. At this time, it is not clear whether a universal threshold can be developed or the optimum threshold will depend on the specific measurement conditions. We also note that plankton layers can be used as a tracer for a number of hydrodynamic effects in the upper ocean.

5. REFERENCES

1. Churnside, J. H., et al., Airborne lidar for fisheries applications, *Opt. Eng.* Vol. 40, 406-414, 2001.

2. American National Standards Institute, *Safe Use of Lasers, Standard Z-136.1,* Laser Institute of America, Orlando, 1993, p. 120.

3. Zorn, H. M., et al., Laser safety thresholds for cetaceans and pinnipeds, *Mar. Mamm. Sci.* Vol. 16, 186-200, 2000.

4. Churnside, J. H., et al., Lidar profiles of fish schools," *Appl. Opt*. Vol. 36, 6011-6020, 1997.

5. Churnside, J. H. and Thorne, R. E. , Comparison of airborne lidar measurements with 420 kHz echo sounder measurements of zooplankton," *Appl. Opt.* Vol. 44, 5504-5511, 2005.

6. Cooney, R. T., et al., Seasonality in surface-layer net zooplankton communities in Prince William Sound, Alaska, *Fish. Ocean*. Vol. 10 (Suppl. 1), 97-109, 2001.

7. Cooney, R. T., Zooplankton, in *The Gulf of Alaska, Physical Environmental And Biological Resources*, D. W. Hood and S. T. Zimmerman, eds., U.S. Interior Department Minerals Management Service, Washington, 1986, pp. 285-304.

8. Willette, T. M. , et al., Ecological processes influencing mortality of juvenile pink salmon (Onchorynchus gorbuscha) in Prince William Sound, Alaska, *Fish. Ocean*. Vol. 10 (Suppl. 1) 14-41, 2001.

9. Cooney, R. T., et al., Ecosystems controls of juvenile pink salmon (*Onchorynchus gorbuscha*) and Pacific herring (*Clupea pallasi*) populations in Prince William Sound, Alaska, *Fish. Ocean*. Vol. 10 (Suppl. 1), 1-13, 2001.

10. Dekshenieks, M. M., et al., Temporal and spatial occurrence of thin phytoplankton layers in relation to physical processes," *Mar. Ecol. Prog. Ser*. Vol. 223, 61-71, 2001.

11. Churnside, J. H. and Ostrovsky, L. A., LIDAR observation of a strongly nonlinear internal wave in the Gulf of Alaska, *Int. J. Remote Sens*. Vol. 26, 167-177, 2005.